Oxidized-CaMKII and *O*-GlcNAcylation cause increased atrial fibrillation in diabetic mice by distinct mechanisms

Olurotimi O. Mesubi[1*], Adam G. Rokita[2,3], Neha Abrol[1], Yuejin Wu[1], Biyi Chen[2], Qinchuan Wang[1], Jonathan M. Granger[1], Anthony Tucker-Bartley[1], Elizabeth D. Luczak[1], Kevin R. Murphy[1], Priya Umapathi[1], Partha S. Banerjee[4], Tatiana N. Boronina[4], Robert N. Cole[4], Lars S. Maier[3], Xander H. Wehrens[5], Joel L. Pomerantz[4,6], Long-Sheng Song[2], Rexford S. Ahima[7], Gerald W. Hart[4], Natasha E. Zachara[4], Mark E. Anderson[1,8,9*].

Supplemental Material

Supplemental Methods

Diabetic mouse models

Type-1 diabetes (T1D) was induced by a single intraperitoneal (i.p.) injection of streptozotocin (STZ) (185mg/kg, Sigma-Aldrich). After a six hour fast, adult (2 – 4 month old) male mice received an i.p. injection of STZ dissolved in a citrate buffer (citric acid and sodium citrate, pH 4.0) or citrate buffer alone for control mice. These mice were maintained on normal chow diet (NCD) (7913 irradiated NIH-31 modified 6% mouse/rat diet – 15 kg, Envigo, Indianapolis, IN) Blood glucose was checked 7 days later with a glucometer via tail vein and mice with blood glucose levels ≥ 300mg/dl were considered diabetic. During the initial period of this study, the TRUEresult (Nipro Diagnostics, FL, USA) glucometer was used for blood glucose checks. However, the manufacture of this glucometer was discontinued and, thus, subsequent glucose checks were performed using the OneTouch Ultra 2 (LifeScan, Zug, Switzerland). STZ-treated mice that had blood glucose levels < 300mg/dl received a second i.p. injection of STZ after a six-hour fast and blood glucose was checked again 7 days after the repeat injection. If blood glucose levels at repeat check was ≥ 300mg/dl, the mice were considered diabetic otherwise they were excluded from the study. Blood glucose, echocardiography and electrophysiology study were done 2 weeks after initiation of STZ injections.

To induce a model of type-2 diabetes (T2D), male mice (C57BL/6J and other mouse genotypes used in this study) aged 5 – 6 weeks were maintained on a high-fat diet (HFD) (Rodent diet with 60 kcal% fat – D12492, Research Diets, New Brunswick, NJ). Five weeks following the initiation of HFD, the mice received daily intraperitoneal (i.p.) injections of low dose streptozocin (STZ) (40 mg/kg/day, Sigma-Aldrich) for three consecutive days after a six hour fast on each day. STZ was dissolved in a citrate buffer (citric acid and sodium citrate, pH 4.0). For control mice, age-matched littermates were maintained on NCD (7913 irradiated NIH-31 modified 6% mouse/rat diet – 15 kg, Envigo, Indianapolis, IN) and received daily i.p. injections of citrate buffer for three consecutive days at similar age as the HFD mice. Blood glucose was checked via tail vein using a glucometer (OneTouch Ultra 2 meter) two weeks after STZ or citrate buffer injection. In addition, body weight, insulin tolerance test, glucose tolerance test and echocardiography were performed two weeks after STZ or citrate buffer injections. Insulin resistance was measured using the Homeostatic Model Assessment of Insulin Resistance (HOMA-IR) calculation based on fasting insulin and glucose levels.

Blood samples for serum chemistries and renal function

To assess for ketoacidosis and renal function, blood samples for serum chemistries – glucose, blood urea nitrogen, creatinine, and carbon dioxide; were obtained 2 weeks after STZ injection in the T1D mice. Blood sample collection was via facial vein puncture and analysis was performed in the mouse phenotyping core.

Insulin therapy

Exogenous insulin was delivered subcutaneously via sustained release insulin implants – LinBit (LinShin, Toronto, ON, Canada) (1, 2) to T1D mice with blood glucose levels > 300 mg/dl, one week after STZ injection. Two to 4 implants were implanted subcutaneously according to the manufacturer's instructions based on the body weight of the mice.

MitoTEMPO and TPP injections

One week after STZ injection, T1D mice received daily i.p. injections (1mg/kg/day) of MitoTEMPO (2-(2,2,6,6-Tetramethylpiperidin-1-oxyl-4-ylamino)-2-oxoethyl) triphenylphosphonium chloride monohydrate, Enzo Life Sciences, Inc., product number: ALX-430-150-M005) or TPP (Formylmethyl)triphenylphosphonium chloride (2-Oxoethyltriphenylphosphonium chloride) for 7 – 10 days.

DON injections

T1D mice received DON (diazo-5-oxonorleucine, 5 mg/kg, i.p.) (3) dissolved in phosphate-buffered saline 30 minutes – 1 hour prior to induction of anesthesia for electrophysiology study and rapid atrial burst pacing.

Mouse electrophysiology and AF induction

In vivo electrophysiology (EP) studies were performed as previously reported with some modifications (4-6) in mice anesthetized with isoflurane (1.5 – 2% for induction and 1 – 2 % for maintenance of anesthesia; Isotec 100 Series Isoflurane Vaporizer; Harvard Apparatus). Mouse core body temperature (monitored by a rectal probe), heart rate and respiratory rate during the procedure were monitored with a heated surgical monitoring system (MouseMonitorTM S, Indus Instruments, USA) and the body temperature was maintained at 37.0 ± 0.5°C. A Millar 1.1F octapolar EP catheter (EPR-800; Millar/ADInstruments, USA) was introduced via the right jugular vein, as previously described (4, 7), into the right atrium and ventricle for recording intracardiac electrograms. A computer-based data acquisition system (Powerlab 16/30; ADInstruments, USA) simultaneously recorded a 3-lead body surface ECG and up to 4 intracardiac bipolar electrograms (Labchart Pro software, version 7, ADInstruments). Right atrial pacing was achieved by delivering 2-ms current pulses by an external stimulator (STG-3008; Multi Channel Systems). AF inducibility was determined by decremental burst pacing. Burst pacing was started at a cycle length of 40ms, decreasing by 2ms every 2 seconds to a cycle length of 8ms. Burst pacing was performed for a total of five times with an interval of one minute after the end of the previous burst protocol or AF termination. AF was defined as the occurrence of rapid and fragmented atrial

electrograms with irregular AV-nodal conduction and ventricular rhythm for at least 1 second. If 1 or more bursts (out of 5) were an AF episode, the mouse was deemed inducible for AF, and non-inducible if there were no AF episodes.

Transthoracic echocardiography

Transthoracic echocardiography was performed in conscious mice using the Sequoia C256 ultrasound system (Malvern, PA) equipped with a 15-MHz linear transducer as previously described (8, 9). Briefly, M-mode echocardiogram was obtained from parasternal views of the left ventricle at the level of the papillary muscles at sweep speed of 200 mm/sec. Left ventricular dimensions were averaged over 3 to 5 beats at physiological heart rates, and left ventricular mass, fractional shortening and ejection fraction were derived. A blinded operator performed image acquisition and analysis.

Human samples

De-identified right atrial tissue samples used for CaMKII isoform expression were obtained from patients undergoing cardiac surgery without atrial fibrillation or diabetes.

Immunoblots

Protein immunodetection by standard western blot techniques was performed.
Briefly, mice were sacrificed 2 – 4 weeks after STZ or citrate injection, hearts were excised, flash frozen in liquid nitrogen and stored at -80^{o}C. Hearts were lysed with 1% Triton buffer containing protease inhibitor (P8340, Sigma), phosphatase inhibitor (P0044, Sigma), Thiamet G (SML0244, Sigma), and PUGNAc (A7229, Sigma). Protein fractionation was performed using Nupage gels (Invitrogen) and transferred to PVDF membranes (Bio-Rad). Blots were incubated with primary antibodies – CaMKII delta (1:1000, catalog ab181052, Abcam), *O*-GlcNAc (1:1000, custom antibody – RL2 from the Hart and Zachara lab) (10, 11), MGEA5/OGA (1:2000, catalog ab124807, Abcam), HA epitope tag (1:1000, catalog 600-401-384), cleaved caspase-3 (1:1000, catalog 9662, Cell Signaling Technology), GAPDH (1:10,000, catalog 5174, Cell Signaling Technology), α/β-Tubulin (1:1000, catalog 2148, Cell Signaling Technology); and subsequently with the appropriate HRP-conjugated secondary antibodies – anti-rabbit (1:10,000, catalog 656120, Invitrogen) IgG and anti-mouse (1:10,000, catalog A8786, Sigma-Aldrich) IgM antibodies. Chemiluminescence with ECL reagent (Lumi-Light, Roche) was used for detection. Densitometric analysis was performed using NIH Image J software and band intensity was normalized to the entire Coomassie-stained gel or GAPDH.

Cellular ROS detection

Hearts were removed immediately after sacrifice, cryopreserved and sectioned at 30-µm thickness. As previously described (12), after washing in phosphate-buffered

saline, heart tissue was pre-incubated with DHE for 30 minutes at 37°C and washed. Fluorescence was detected with a laser scanning confocal microscope (Zeiss 510, 40x oil immersion lens) with excitation at 488 nm and detection at 585 nm. The same scanning parameters were applied to all samples and image analysis was done using NIH Image J software.

Mitochondrial ROS detection

Isolated cardiomyocytes were incubated for 30 minutes with 5µM MitoSOX Red (ThermoFischer Scientific) and 100nM Mitotracker Green (ThermoFischer Scientific). After washing the cells, fluorescence was detected with a laser scanning confocal microscope (Zeiss 510, 40x oil immersion lens). MitoSOX Red (excitation at 510 nm and emission at 580 nm), MitoTracker Green (excitation at 490 nm and emission at 516 nm). Fluorescence was assessed from at least 20 cells in the cell suspension from each mouse. The same scanning parameters were applied to all samples and image analysis was done using NIH Image J software.

Quantitative PCR for CaMKII isoforms

Total RNA from mouse and human atrial tissue was extracted using Trizol reagent (Invitrogen) according to the manufacturer's instructions. After first strand cDNA synthesis, messenger RNA expression was analyzed by quantitative real-time polymerase chain reaction on a BioRad CFX machine using pre-validated primers with SsoAdvanced Universal SYBR Green Supermix (Bio-Rad). GAPDH and HPRT gene expression were used as the reference genes and the specificity of the assay was confirmed by melting curve analysis.

Neonatal mouse cardiomyocyte isolation, culture and transfection

Cardiomyocytes were isolated from hearts excised from neonatal mice (postnatal day 0 – 3), pooled and dissociated using the MACS Neonatal Heart Dissociation Kit (Catalog #130-098-373), Neonatal Cardiomyocyte Isolation kit, mouse (Catalog #130-100-825) and automated gentleMACS Dissociator (Miltenyl Biotec GmbH), according to the manufacturer's instructions (13, 14). After isolation, neonatal mouse cardiomyocytes were suspended in Medium-199 (5.5 mM glucose) supplemented with 10% fetal bovine serum, 25 mM HEPES, 50 U/ml penicillin-streptomycin, 2 ug/ml vitamin B12, and 0.1 mM MEM nonessential amino acids. The neonatal cardiomyocytes were plated on 20 µg/ml fibronectin-coated 35 mm glass bottom culture dishes with 20 mm micro-wells (Cellvis, catalog # D35-20-1.5-N) at a seeding density of 1.0×10^6 cells/dish and incubated overnight at 37 ^{o}C and 5% CO_2. The media was changed the next day from to 2% fetal bovine serum media (Medium-199 as described above).

In-Gel Proteolysis for mass spectrometry

Proteins in gel bands, amount 1 µg, were reduced with 1.5 mg/mL dithiothreitol (DTT) in 50 µL of 50 mM of tri-ethyl ammonium bicarbonate (TEAB) buffer at 57 °C for 45min, then alkylated with 10 mg/mL iodoacetomide in 50 µL of 50 mM TEAB buffer in the dark at room temperature for 30 minutes. Buffers were removed by two alternating washes of 50 mM TEAB and acetonitrile re-swelled on ice with 12.5 ng/µL trypsin (Promega, catalog # V5111) in 40 µL of 50 mM TEAB, and proteolyzed at 37 °C overnight, as previously described by Shevchenko et al. (15). Peptides were extracted with 50% acetonitrile/0.1% TFA, dried, resuspended in 0.1% TFA and desalted on Oasis u-HLB plates (Waters, Milford, MA). Peptides were eluted from Oasis plates with 60% acetonitrile/0.1% TFA, dried by vacuum centrifugation, then resuspended in 2% acetonitrile/0.1% formic acid. 30% of samples were used to identify proteins by data-dependent liquid chromatography tandem mass spectrometry (LC-MS/MS).

LC-MS/MS analysis

Desalted tryptic peptides, were analyzed by nano-liquid chromatography tandem mass spectrometry (nano LC-MS/MS) on an Orbitrap-Lumos mass spectrometer (Thermo Fisher Scientific) interfaced with nano-Acquity LC system (Waters, Milford, MA) using a 2% - 90% acetonitrile/0.1% FA gradient over 70 minutes at 300nl/min on 75 um x 150 mm reverse-phase column (ProntoSIL 120-5-C18 H column 3 µm, 120Å (Bischoff, catalog # F185PS030). Eluting peptides were sprayed into the mass spectrometer through 1 µm emitter tip (New Objective, Woburn, MA) at 2.4 kV. Data dependent analysis was performed by monitoring the top 15 precursor ions in survey scans (350-1800 Da m/z) using a 15s dynamic exclusion. Each prescursor ion was individually isolated with 1.2 Da and fragmented (MS/MS) using HCD activation collision energy 30. Precursor and the fragment ions were analyzed in the orbitrap with resolutions at 200 Da of 120,000 and 30,000, automatic gain control (AGC) targets of $3xe^6$ and $1xe^5$, and maximum injection times (IT) of 60 ms and 200 ms, respectively. Targeted LC-MS/MS analysis was performed under the same chromatography and mass spectrometry conditions. However, instead of monitoring the top 15 precursor ions, a list of m/z values of the STVASMMHR peptide with variable methionine oxidation, serine and threonine O-GlcNAcylation or phosphorylation were monitored, isolated and fragmented.

Mass spectrometry data analysis

Tandem mass spectra were processed by Proteome Discoverer, v.2.3 (ThermoFisher Scientific) using file re-calibration option and analyzed with Mascot, v.2.6.1 (Matrix Science, London, UK) using Percolator (16) for peptide-spectrum matches (PSM) validation. The Mascot database searches were performed using the RefSeq2017_83_Human with the following criteria: trypsin as enzyme, 2 missed cleavage, 4 ppm precursor mass tolerance, 0.01 Da fragment mass tolerance, and the following variable modifications: oxidation on mehtionine, carbamidomethyl on cysteine, deamidation on asparagine or glutamine, phosphorylation or HexNAcylation on serine or threonine. Tandem mass spectra were also analyzed using PEAKS (v10, Bioinformatics Solutions, Inc.) and Byonic (Protein Metrics) against the same

RefSeq2017_83_mus_musculus_database, using the same search criteria as with Mascot, except with mass tolerance of 5 ppm and 0.02 Da on precursor and fragment ions, respectively, in PEAKS and mass tolerances of 5 ppm and 20 ppm on precursor and fragment ions, respectively, in Byonic.

Calcium imaging in isolated atrial myocytes

Calcium imaging of isolated atrial myocytes was performed as described previously (4, 17).

Isolated atrial myocyte action potential recording

Voltage clamp studies using the perforated patch configuration on isolated atrial myocytes were performed as described previously to record single cell action potentials (4, 18).

Fibrosis detection and quantification

Mouse hearts were formalin fixed and paraffinized and four chamber heart sections were cut along the coronal plane. Heart sections were deparaffinized through xylene, 100% ethanol, 95% ethanol and then water. The slides were stained using a Masson's Trichrome Aniline Blue Stain KIT (Newcomer Supply, 9179B) to assess for fibrosis in atrial tissue. The images were digitalized and imaged at 20x magnification with an Aperio Scanscope CS. The images were analyzed semi-automatically using Aperio ImageScope software (Aperio Technologies/Leica Biosystems), with a lower intensity threshold of 150 and a hue value of 0.66. All atrial myocardium was included with perivascular fibrous tissue.

References

1. Wang PY. Palmitic acid as an excipient in implants for sustained release of insulin. *Biomaterials.* 1991;12(1):57-62.
2. Ohzato H, Porter J, Monaco AP, Montana E, and Maki T. Minimum number of islets required to maintain euglycemia and their reduced immunogenicity after transplantation into diabetic mice. *Transplantation.* 1993;56(2):270-4.
3. Erickson JR, Pereira L, Wang L, Han G, Ferguson A, Dao K, Copeland RJ, Despa F, Hart GW, Ripplinger CM, et al. Diabetic hyperglycaemia activates CaMKII and arrhythmias by O-linked glycosylation. *Nature.* 2013;502(7471):372-6.
4. Purohit A, Rokita AG, Guan X, Chen B, Koval OM, Voigt N, Neef S, Sowa T, Gao Z, Luczak ED, et al. Oxidized Ca(2+)/calmodulin-dependent protein kinase II triggers atrial fibrillation. *Circulation.* 2013;128(16):1748-57.
5. Chelu MG, Sarma S, Sood S, Wang S, van Oort RJ, Skapura DG, Li N, Santonastasi M, Muller FU, Schmitz W, et al. Calmodulin kinase II-mediated sarcoplasmic reticulum Ca2+ leak promotes atrial fibrillation in mice. *J Clin Invest.* 2009;119(7):1940-51.
6. Verheule S, Sato T, Everett Tt, Engle SK, Otten D, Rubart-von der Lohe M, Nakajima HO, Nakajima H, Field LJ, and Olgin JE. Increased vulnerability to atrial fibrillation in transgenic mice with selective atrial fibrosis caused by overexpression of TGF-beta1. *Circ Res.* 2004;94(11):1458-65.
7. Sood S, Chelu MG, van Oort RJ, Skapura D, Santonastasi M, Dobrev D, and Wehrens XH. Intracellular calcium leak due to FKBP12.6 deficiency in mice facilitates the inducibility of atrial fibrillation. *Heart Rhythm.* 2008;5(7):1047-54.
8. Olson LE, Bedja D, Alvey SJ, Cardounel AJ, Gabrielson KL, and Reeves RH. Protection from doxorubicin-induced cardiac toxicity in mice with a null allele of carbonyl reductase 1. *Cancer Res.* 2003;63(20):6602-6.
9. Wei H, Bedja D, Koitabashi N, Xing D, Chen J, Fox-Talbot K, Rouf R, Chen S, Steenbergen C, Harmon JW, et al. Endothelial expression of hypoxia-inducible factor 1 protects the murine heart and aorta from pressure overload by suppression of TGF-beta signaling. *Proc Natl Acad Sci U S A.* 2012;109(14):E841-50.
10. Holt GD, Snow CM, Senior A, Haltiwanger RS, Gerace L, and Hart GW. Nuclear pore complex glycoproteins contain cytoplasmically disposed O-linked N-acetylglucosamine. *J Cell Biol.* 1987;104(5):1157-64.
11. Snow CM, Senior A, and Gerace L. Monoclonal antibodies identify a group of nuclear pore complex glycoproteins. *J Cell Biol.* 1987;104(5):1143-56.
12. He BJ, Joiner ML, Singh MV, Luczak ED, Swaminathan PD, Koval OM, Kutschke W, Allamargot C, Yang J, Guan X, et al. Oxidation of CaMKII determines the cardiotoxic effects of aldosterone. *Nat Med.* 2011;17(12):1610-8.
13. Trantidou T, Terracciano CM, Kontziampasis D, Humphrey EJ, and Prodromakis T. Biorealistic cardiac cell culture platforms with integrated monitoring of extracellular action potentials. *Sci Rep.* 2015;5(11067.
14. Papanicolaou KN, Ashok D, Liu T, Bauer TM, Sun J, Li Z, da Costa E, D'Orleans CC, Nathan S, Lefer DJ, et al. Global knockout of ROMK potassium channel worsens cardiac

ischemia-reperfusion injury but cardiomyocyte-specific knockout does not: Implications for the identity of mitoKATP. *J Mol Cell Cardiol.* 2020;139(176-89.
15. Shevchenko A, Wilm M, Vorm O, and Mann M. Mass spectrometric sequencing of proteins silver-stained polyacrylamide gels. *Anal Chem.* 1996;68(5):850-8.
16. Kall L, Canterbury JD, Weston J, Noble WS, and MacCoss MJ. Semi-supervised learning for peptide identification from shotgun proteomics datasets. *Nat Methods.* 2007;4(11):923-5.
17. Guatimosim S, Guatimosim C, and Song LS. Imaging calcium sparks in cardiac myocytes. *Methods Mol Biol.* 2011;689(205-14.
18. Wu Y, Gao Z, Chen B, Koval OM, Singh MV, Guan X, Hund TJ, Kutschke W, Sarma S, Grumbach IM, et al. Calmodulin kinase II is required for fight or flight sinoatrial node physiology. *Proc Natl Acad Sci U S A.* 2009;106(14):5972-7.

Supplemental Tables

Supplementary Table 1. Cardiac morphometric measures and serum chemistry of WT Ctrl and T1D mice at electrophysiology study.

	WT Ctrl	**WT T1D**
Heart weight/tibial length (mg/mm)	6.85 ± 0.18, n=6	4.93 ± 0.15, n=9*
Atrial weight/tibial length (mg/mm)	0.53 ± 0.03, n=6	0.38 ± 0.02, n=9*
Ventricular weight/tibial length (mg/mm)	6.18 ± 0.20, n=6	4.43 ± 0.15, n=9*
CO_2	15.5 ± 1.1	16.8 ± 0.7
BUN (mg/dl)	24.6 ± 0.7	24.2 ± 1.7
Cr (mg/dl)	0.4 ± 0	0.4 ± 0.03
Serum blood glucose (mg/dl)	183.4 ± 13.4	697.4 ± 48.42*

Heart weight normalized to tibial length, atrial weight normalized to tibial length, and ventricular weight normalized to tibial length (*$p < 0.05$); n = 6 – 9/group. Serum pCO2, BUN, creatinine and blood glucose. (*$p < 0.05$, n = 4 – 5/group). Data are means ± s.e.m

Supplementary Table 2. Patient characteristics for atrial samples.

Patient Characteristics	**Sinus rhythm and no DM (n = 5)**
Age (year)	68 ± 4
Male:Female	2:3
Ejection Fraction (%)	57 ± 9
Drug Treatment	
B-blocker, n (%)	4/5 (80)
ACEI/ARB, n (%)	5/5 (100)
Calcium channel blocker, n (%)	0/5 (0)
Statin, n (%)	5/5 (100)

ACEI, Angiotensin converting enzyme inhibitor; ARB – Angiotensin receptor blocker.

Supplementary Table 3. Coverage of CaMKII isoforms in mass spectrometric analysis of heart lysate samples

Assession Number	Protein	Percent Coverage	Unique Peptides	O-GlcNAc Sites Identified	Phosphorylation Sites Identified	Engine
XP_017174906	CaMKII delta isoform X8 (X7, X12, others)	57.7	4 (64)	no	S276, T277, T287	Byonic, PEAKS
XP_017174906	CaMKII delta isoform X8 (X7, X12, others)	57.7	4 (64)	no	S276, T277 S280, T287	PD-Mascot-Percolator
XP_006518551.1	CaMKII gamma isoform X1 (X7)	53.4	4	no	S280, T287	Byonic (Pep 3e-8)
XP_006518557.1	CaMKII gamma isoform X7 (X6)	46.2	4 (35)	no	S280, T287	PD-Mascot-Percolator, Byonic (PEP 1.4e-19)
XP_006540759.1	PREDICTED: nucleobindin-1 isoform X1	32%	13	S38/T42/T44	none	PD-Mascot-Percolator; Byonic

Supplementary Table 4. Calculated b and y fragment ions of STVASMMHRQETVECLR with phosphorylation on S280 and T287 and oxidation on M281 and M282. Red m/z values are present in Supplementary Figures 5A and 5B within <0.01 m/z.

#	a calc.	b calc.	b-18 calc.	b++ calc.	Seq	y calc.	y++ calc.	#
1	60.0444	88.0393	70.0287	44.5233	S			17
2	161.0921	189.087	171.0764	95.0471	T	2082.8208	1041.914	16
3	260.1605	288.1554	270.1448	144.5813	V	1981.7731	991.3902	15
4	331.1976	359.1925	341.1819	180.0999	A	1882.7047	941.856	14
5	498.196	526.1909	508.1803	263.5991	S(+79.97)	1811.6676	906.3374	13
6	645.2314	673.2263	655.2157	337.1168	M(+ 15.99)	1644.6692	822.8382	12
7	792.2668	820.2617	802.2511	410.6345	M(+ 15.99)	1497.6338	749.3205	11
8	929.3257	957.3206	939.31	479.1639	H	1350.5984	675.8028	10
9	1085.427	1113.422	1095.411	557.2145	R	1213.5395	607.2734	9
10	1213.485	1241.48	1223.47	621.2438	Q	1057.4384	529.2228	8
11	1342.528	1370.523	1352.512	685.7651	E	929.3798	465.1935	7
12	1523.542	1551.537	1533.526	776.2721	T(+ 79.97)	800.3372	400.6722	6
13	1622.61	1650.605	1632.595	825.8063	V	619.3232	310.1652	5
14	1751.653	1779.648	1761.637	890.3276	E	520.2548	260.631	4
15	1854.662	1882.657	1864.647	941.8322	C	391.2122	196.1097	3
16	1967.746	1995.741	1977.731	998.3742	L	288.203	144.6051	2
17					R	175.119	88.0631	1

Supplementary Table 5. Calculated b and y fragment ions of STVASMMHRQETVECLR with phosphorylation on S276 and T287 and oxidation on M281 and M282. Red m/z values are present in Supplementary Figures 5A and 5C within <0.01 m/z.

#	Immonium	b	b-NH3	b (2+)	Seq	y	y-NH3	Y (2+)	#
1	140.011	168.006	150.979	84.503	S(+ 79.97)				17
2	74.061	269.054	252.027	135.027	T	2002.854	1985.828	1001.927	16
3	72.081	368.122	351.095	184.561	V	1901.810	1884.780	951.403	15
4	44.050	439.159	422.132	220.080	A	1802.738	1785.711	901.875	14
5	60.045	526.191	509.164	263.596	S	1731.704	1714.674	866.351	13
6	120.048	673.227	656.200	337.113	M(+ 15.99)	1644.669	1627.642	822.835	12
7	120.048	820.262	803.235	410.631	M(+ 15.99)	1497.634	1480.6071	749.317	11
8	110.072	957.321	940.294	479.161	H	1350.598	1333.571	675.799	10
9	129.114	1113.422	1096.395	557.211	R	1213.539	1196.512	607.270	9
10	101.071	1241.481	1224.454	621.240	Q	1057.438	1040.411	529.219	8
11	102.055	1370.523	1353.496	685.762	E	929.380	912.353	465.190	7
12	154.027	1551.537	1534.510	776.269	T(+ 79.97)	800.337	783.310	400.669	6
13	72.081	1650.606	1633.579	825.803	V	619.325	602.296	310.162	5
14	102.055	1779.648	1762.621	890.324	E	520.256	503.228	260.627	4
15	76.022	1882.658	1865.631	941.829	C	391.213	374.186	196.106	3
16	86.097	1995.742	1978.715	998.371	L	288.203	271.176	144.602	2
17	129.114				R	175.119	158.092	88.059	1

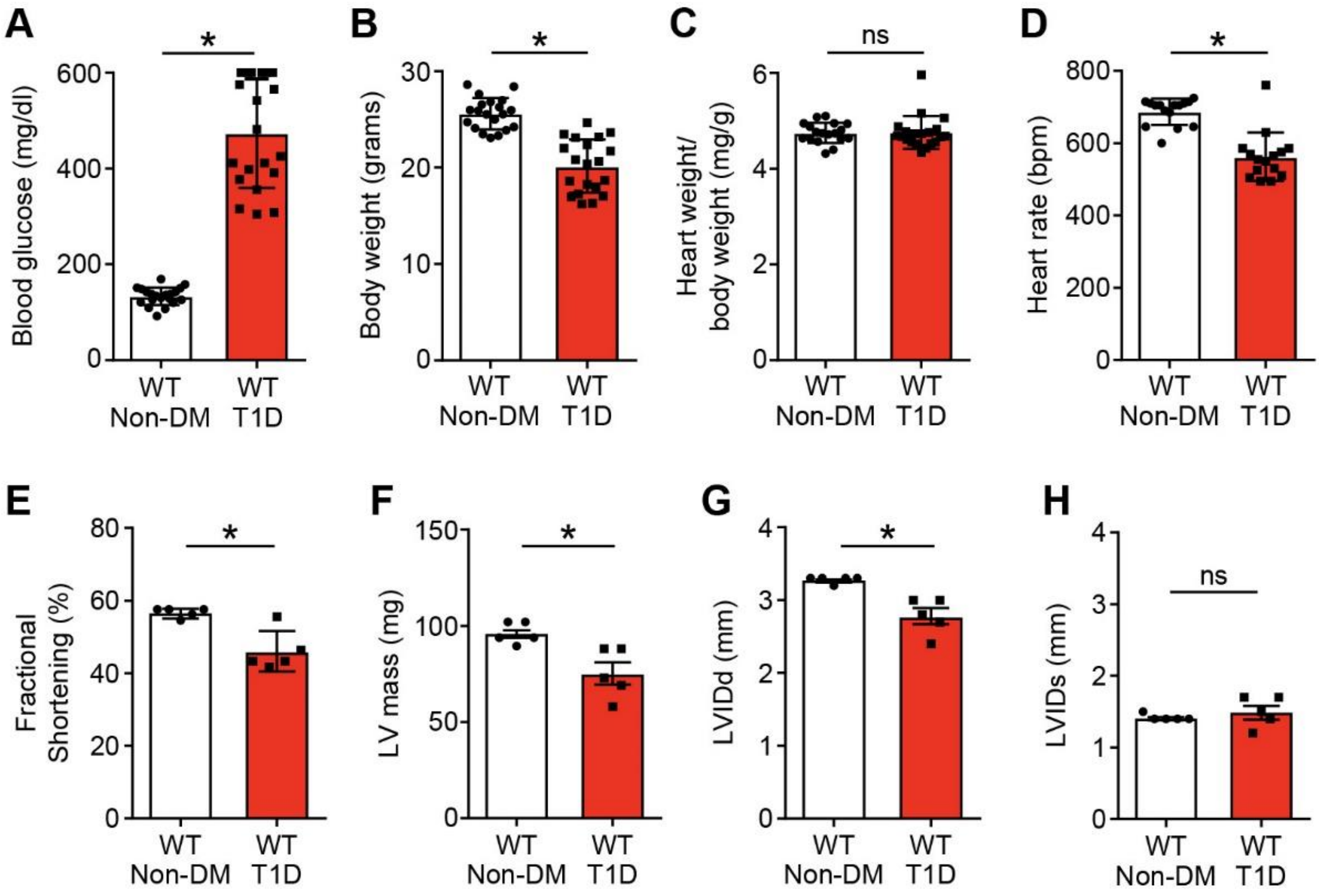

Figure S1. T1D mouse model

Summary data for (A) blood glucose and (B) body weight one week after STZ injection (n = 20 WT non-DM, n = 20 WT T1D); Summary data for (C) heart weight indexed for body weight and (D) heart rate two weeks after STZ injection (n = 18 WT non-DM, n = 20 WT T1D); Summary data of echocardiographic parameters two weeks after STZ injection – fractional shortening (E), LV mass (F), LVIDd (G) and LVIDs (H) in WT non-DM (n = 5) and WT T1D (n = 5). LV, left ventricular; LVIDd, LV internal diameter end diastole; LVIDs, LV internal diameter end systole; STZ, streptozocin. Data are represented as mean ± s.e.m., significance was determined using two-tailed Student's t test (A – H). (*$p < 0.05$, ns – not significant).

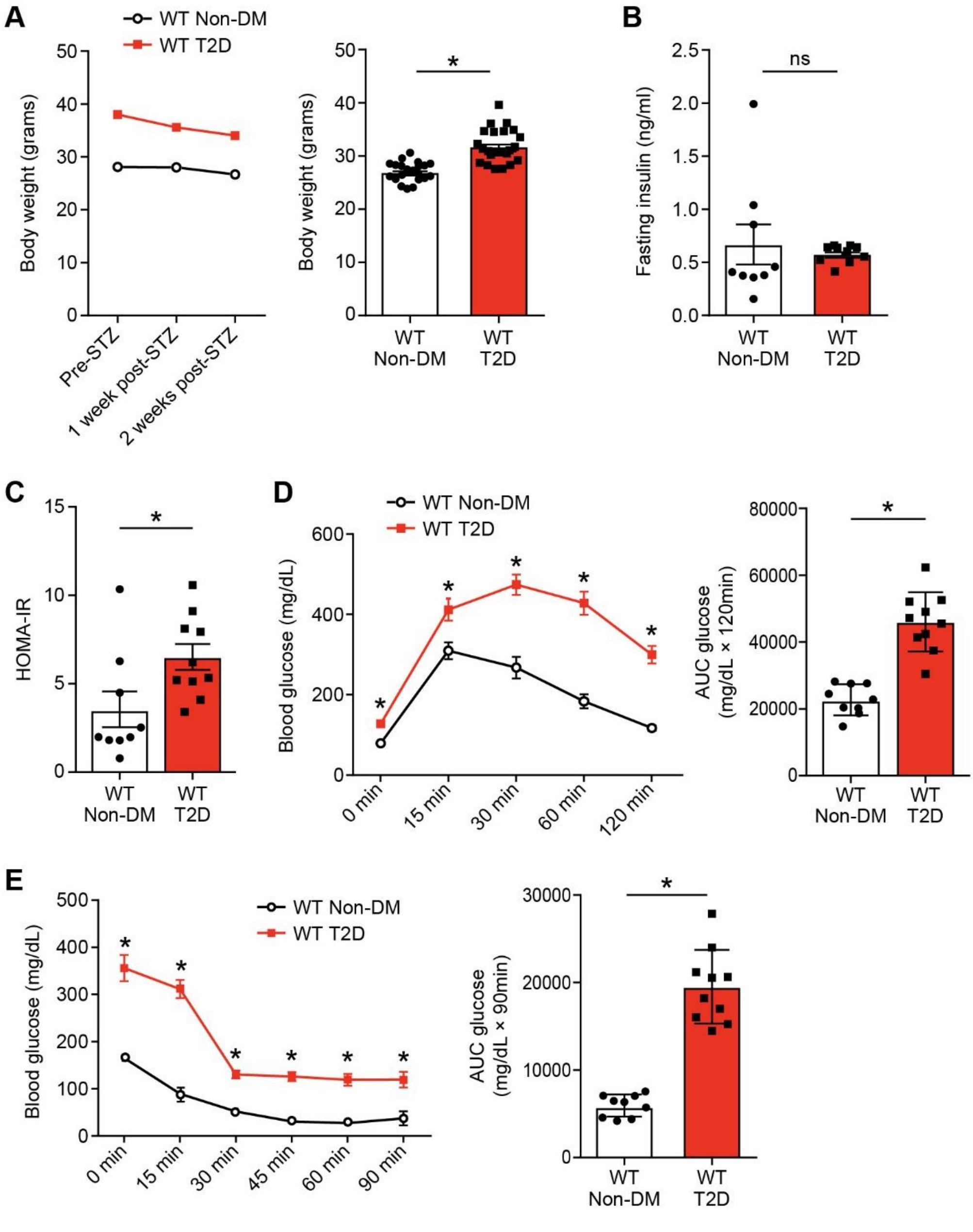

Figure S2. T2D mouse model

Summary data for (A) body weight trend (left panel) after five weeks of high-fat diet and subsequent daily doses of low dose STZ for three consecutive days (n = 7 WT non-DM, n = 10 WT T2D), and body weight (right panel) two weeks of after STZ injection at time of EP study (n = 21 WT non-DM, n = 24 WT T2D) (B) Summary data for fasting insulin level in WT non-DM and T2D mice two weeks after STZ injection; T2D mice had features consistent with T2D as determined by homeostatic model assessment of insulin resistance, HOMA-IR (C), glucose tolerance test (D) and insulin tolerance test (E) (n = 9 WT non-DM, n = 10 WT T2D). AUC, area under the curve; GTT, glucose tolerance test; ITT, insulin tolerance test. Data are represented as mean ± s.e.m.; significance was determined using two-tailed Student's t test (A – E). (*$p < 0.05$, ns – not significant).

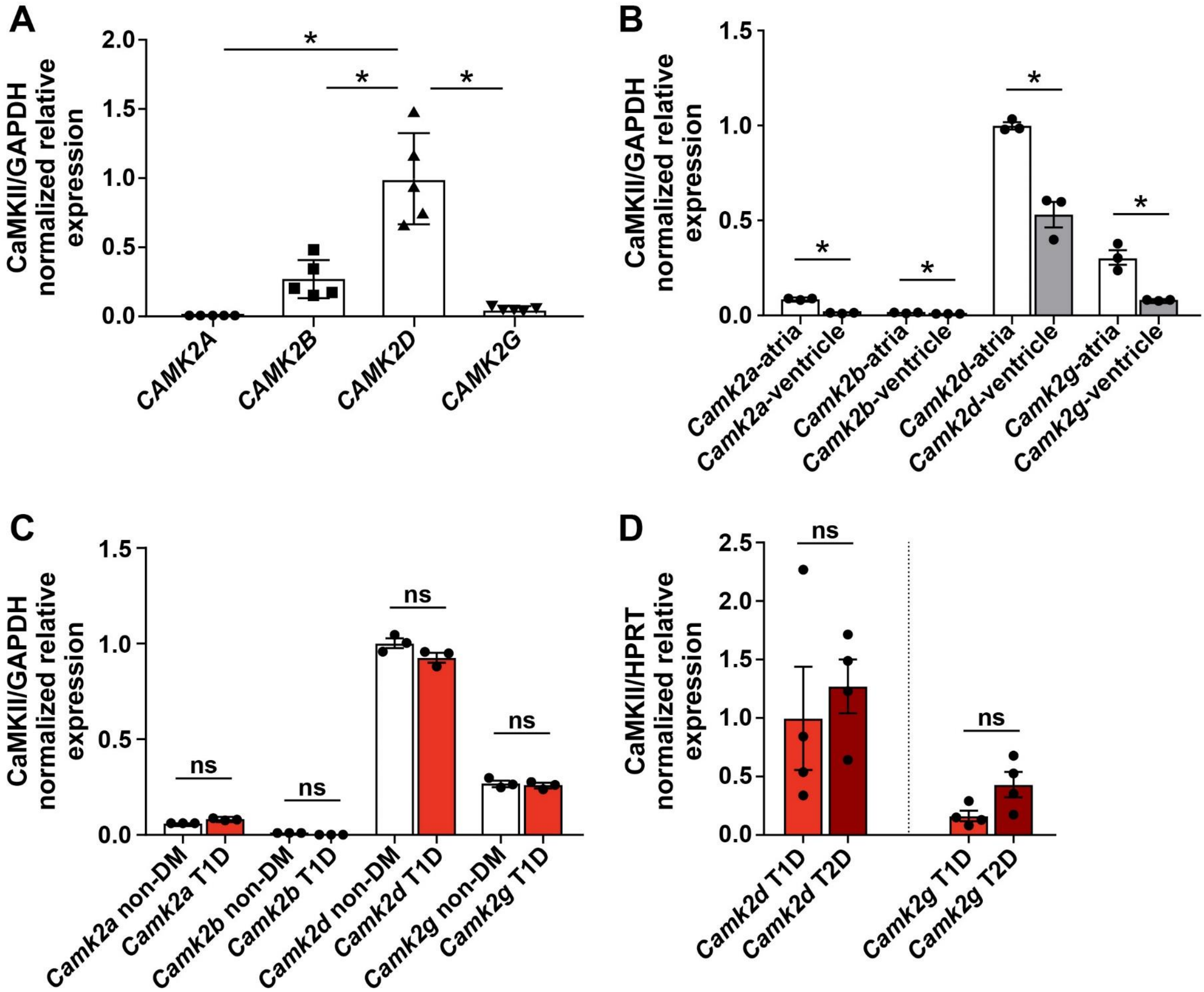

Figure S3. CaMKIIδ is the predominant isoform in human and mouse atria.
(A) CaMKII isoforms (*A, B, D,* and *G*) mRNA expression in human atria from non-diabetic patients with no history of AF measured by qRT-PCR using total RNA (n = 5). See Supplemental Table 2 for patient characteristics. (B) CaMKII isoforms (*a, b, d,* and *g*) mRNA expression in atria and ventricles from WT non-diabetic mice measured by qRT-PCR using total RNA (n = 5). (C) CaMKII mRNA expression in atria from non-diabetic and WT T1D mice (n = 5 WT non-DM, n = 5 WT T1D). (D) *Camk2g* and *Camk2d* mRNA expression in atria from WT T1D compared with WT T2D mice (n = 4 WT T1D, n = 4 WT T2D). Data are represented as mean ± s.e.m. Statistical comparisons were performed using one-way AVOVA with Tukey's multiple comparisons post-hoc test (A) and two-tailed Student's t test (B, C and D). (*$p < 0.05$, ns – not significant).

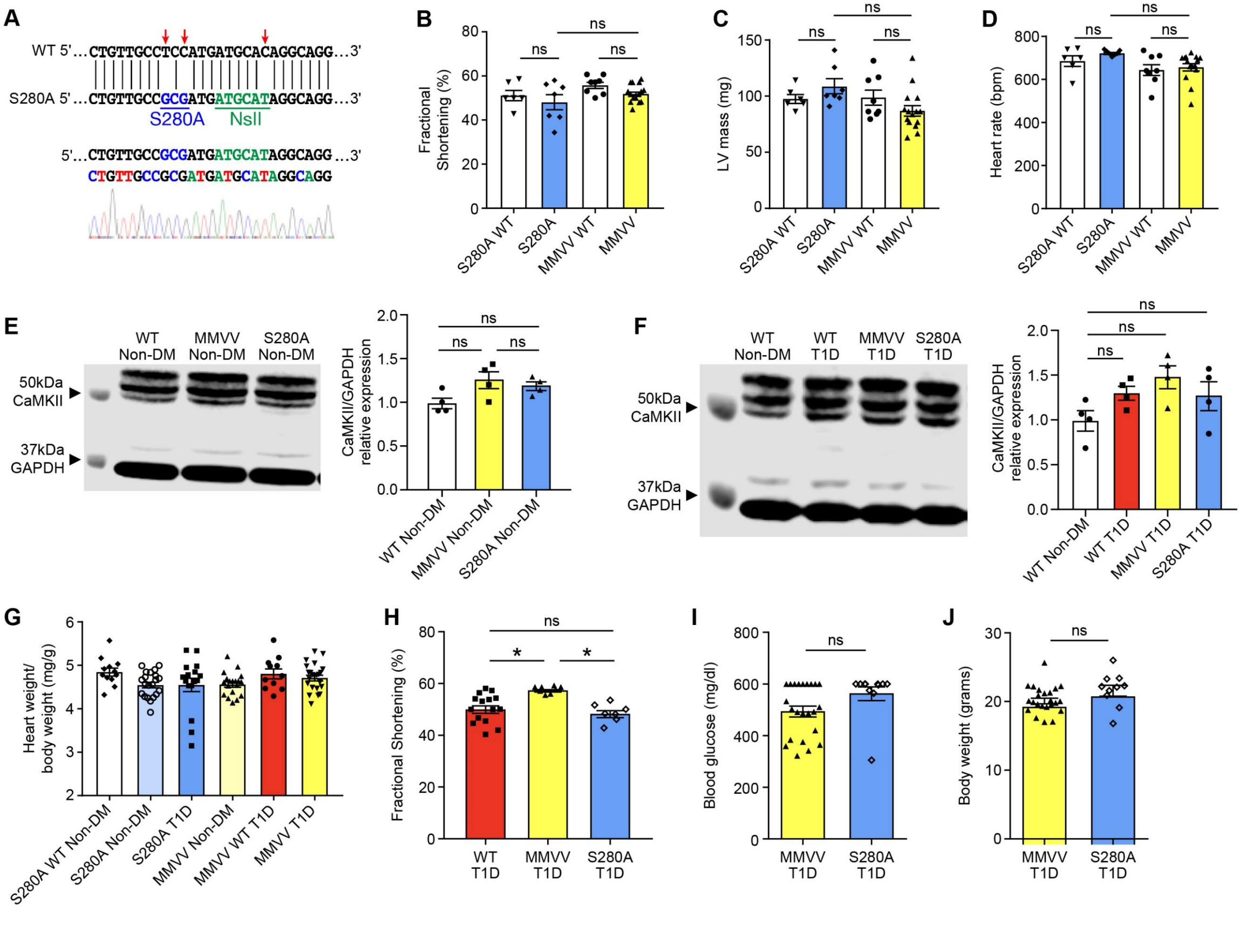

Figure S4. Characteristics of S280A and MMVV mice

(A) Design of knock-in sequence and NsiI genotyping site for S280A mice. Summary data for echocardiographic analysis of non-diabetic S280A and MMVV mice revealed no difference in fractional shortening (B), LV mass (C) or heart rate (D) compared to WT littermates (n = 6 S280A WT, n = 7 S280A, n = 8 MMVV WT, n = 15 MMVV). (E) Representative western blot (left panel) and summary data (right panel) for CaMKII and GAPDH in heart lysates from non-DM WT (n = 4), MMVV (n = 4) and S280A (n = 4) mice. (F) Representative western blot (left panel) and summary data (right panel) for CaMKII and GAPDH in heart lysates from WT non-DM (n = 4), T1D WT (n = 4), MMVV (n = 4), and S280A (n = 4) mice. (G) Summary data for heart weight indexed for body weight in non-diabetic and T1D S280A and MMVV mice and WT littermate controls (n = 12 S280A WT non-DM, n = 21 S280A non-DM, n = 16 S280A T1D, n = 19 MMVV non-DM, n = 11 MMVV WT T1D, n = 23 MMVV T1D). (H) Summary data for LV fractional shortening in T1D WT, MMVV and S280A mice. MMVV mice were protected from diabetic cardiomyopathy compared to T1D WT and MMVV mice (n = 15 WT T1D, n = 23 MMVV T1D, n = 11 S280A T1D). Summary data for blood glucose (I) and body weight (J) in T1D MMVV and S280A mice, two weeks after STZ injection (n = 23 MMVV T1D, n = 10 S280A T1D). Data are represented as mean ± s.e.m., statistical comparisons were performed using one-way AVOVA with Tukey's multiple comparison's test (B – H) and two-tailed Student's t test (I and J). (*p <0.05 ns – not significant).

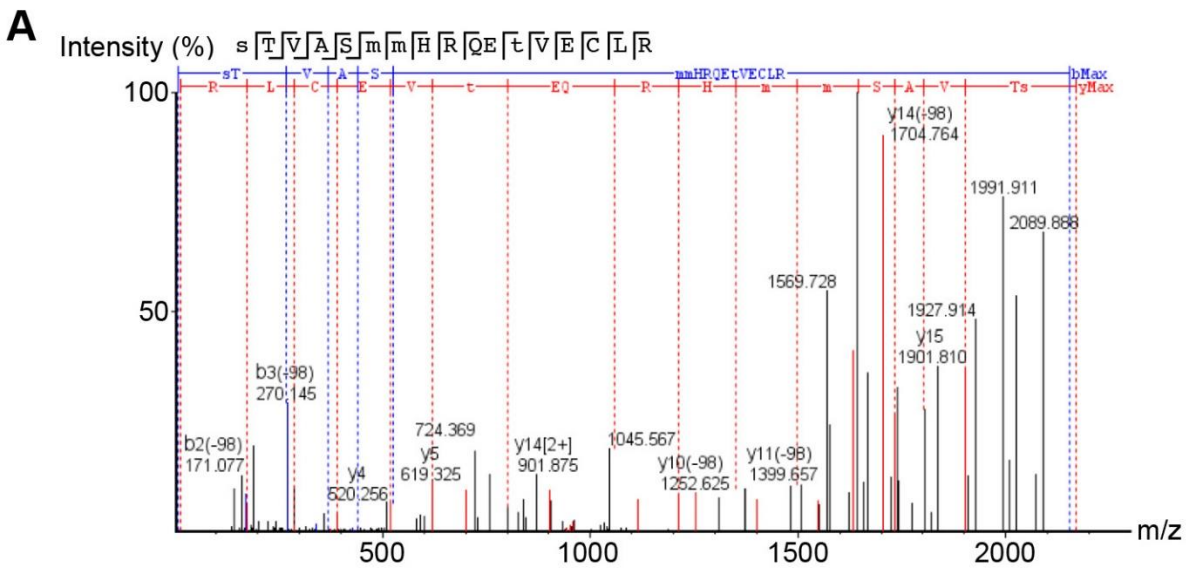

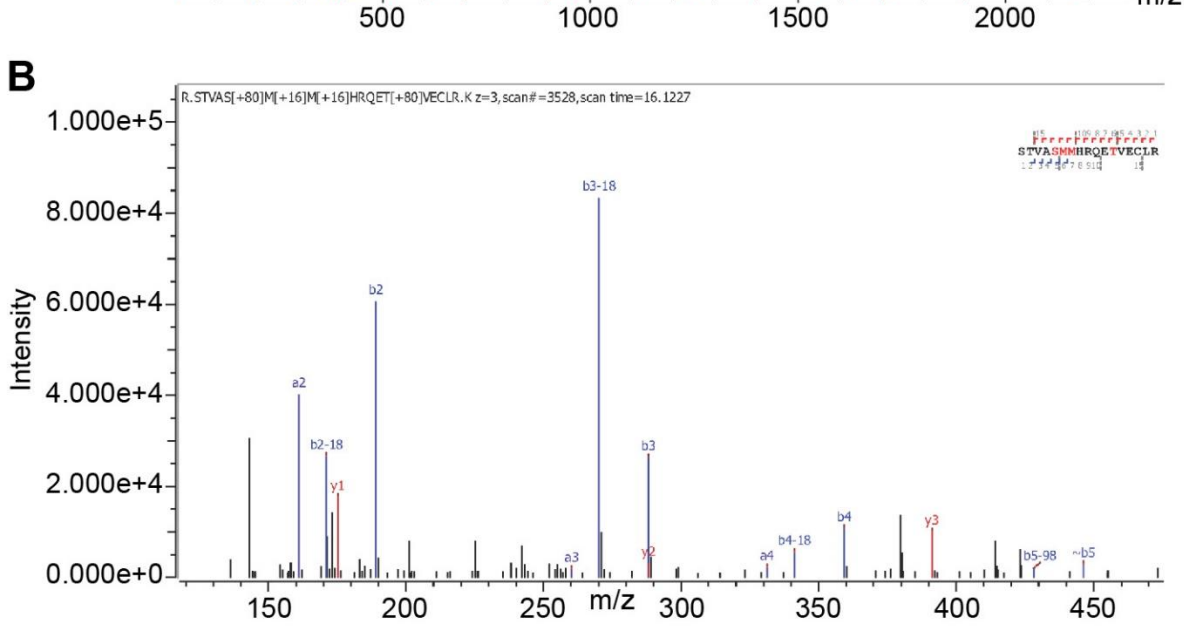

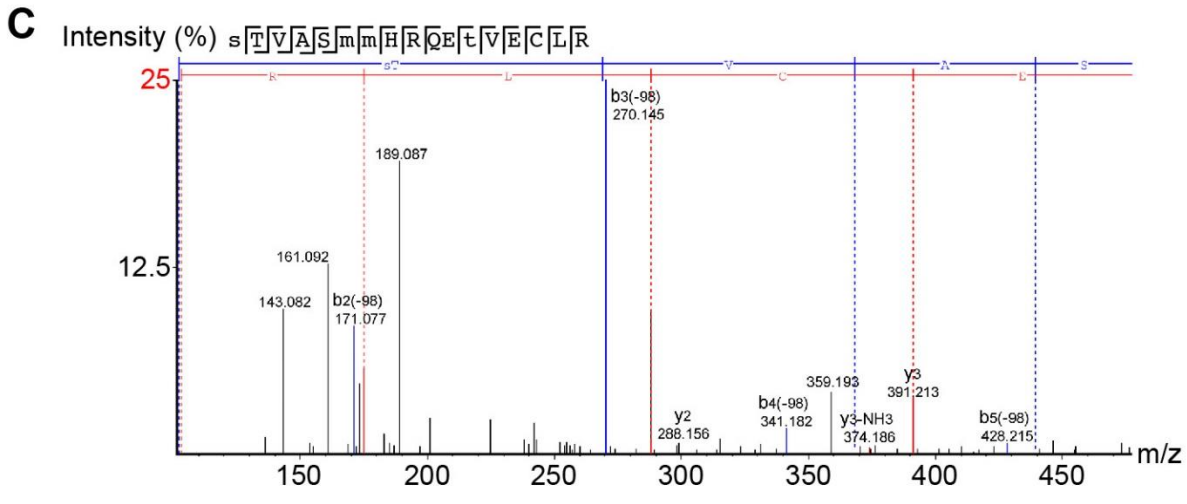

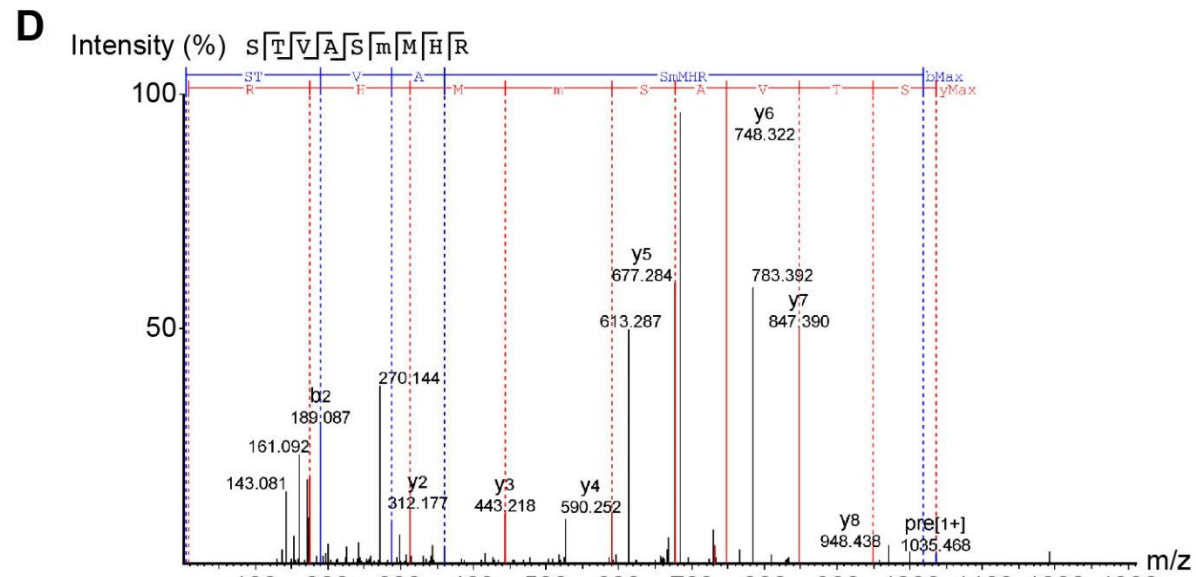

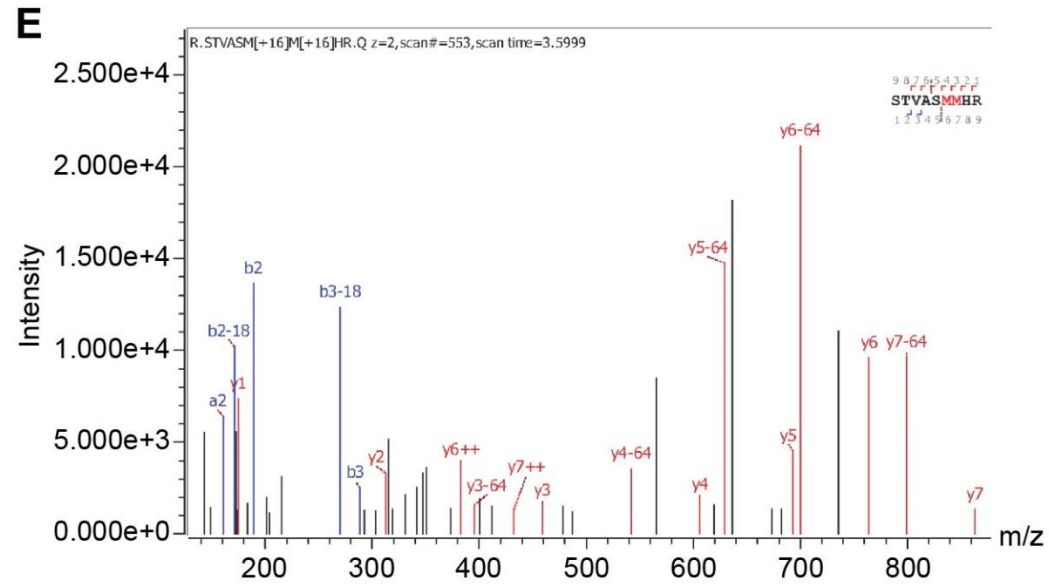

Figure S5. Tandem MS analysis showed phosphorylation but no OGN at S280, and confirmed oxidation at MM281/282 and phosphorylation at T287 in diabetic hearts.

Heart lysates from non-diabetic and diabetic hearts were subjected to in-gel proteolysis followed by LC-MS/MS analysis with a focus on the peptide – STVASMMHR. The observed fragment ions are indicated in the sequence for each spectra. Small case letters and red letters indicate fragment ions that contain the mass shift indicative of the respective modifications (A) Fragmentation of di-phosphorylated and di-oxidized STVASMMHRQETVECLR shows phosphorylation at S276 and T287, and oxidization at M281 and M282. A neutral loss of -98 Da (H_3PO_4) represents loss of the phosphate group plus water from Ser or Thr and the loss of -64 Da represents the loss of the oxidized sulfate group from methionine. (B) Expanded m/z range from spectra in A showing b3 ion which maps phosphorylation to S280 and (C) a 270.145 m/z ion that is either b3-18 (loss of H_2O) if phosphate is on S280 or b3-98 (loss of H_3PO_4) if phosphate is at S276 or T277, and is consistent with a chimera spectrum containing both di-phosphorylated forms of this peptide. Fragmentation spectra show STVASMMHR is oxidized at M281 (D) and di-oxidized at M281 and M282 (E).

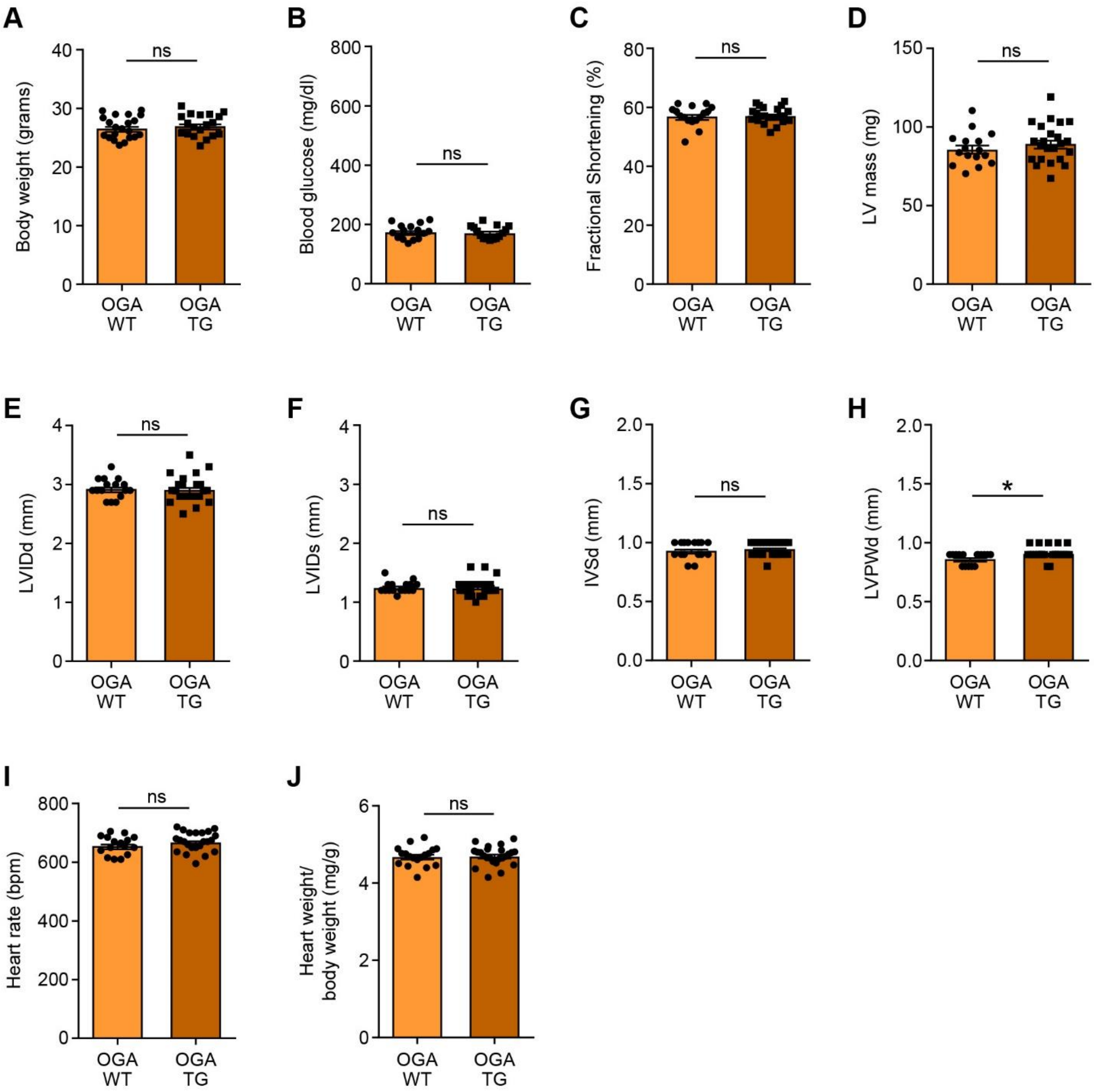

Figure S6. Cardiac phenotyping of OGA-TG mice

(A) Summary data for body weight in WT (n = 21) and OGA-TG (n = 19) mice. (B) Summary data for baseline blood glucose in non-diabetic WT (n = 15) and OGA-TG (n = 15) mice. Summary data of echocardiographic parameters in non-diabetic WT (n = 16) and OGA-TG (n = 23) mice – LV fractional shortening (C), LV mass (D), LVIDd (E), LVIDs (F), IVSd (G), LVPWd (H) and heart rate (I). There were no differences in any of these parameters. (J) Summary data for heart weight indexed for body weight in WT (n = 18) and OGA-TG (n = 24). IVSd, interventricular septal end diastolic dimension; LVPWd, left ventricular posterior wall end diastolic dimension. Data are represented as mean ± s.e.m., statistical comparisons were performed using two-tailed Student's t test. (*p <0.05, ns – not significant).

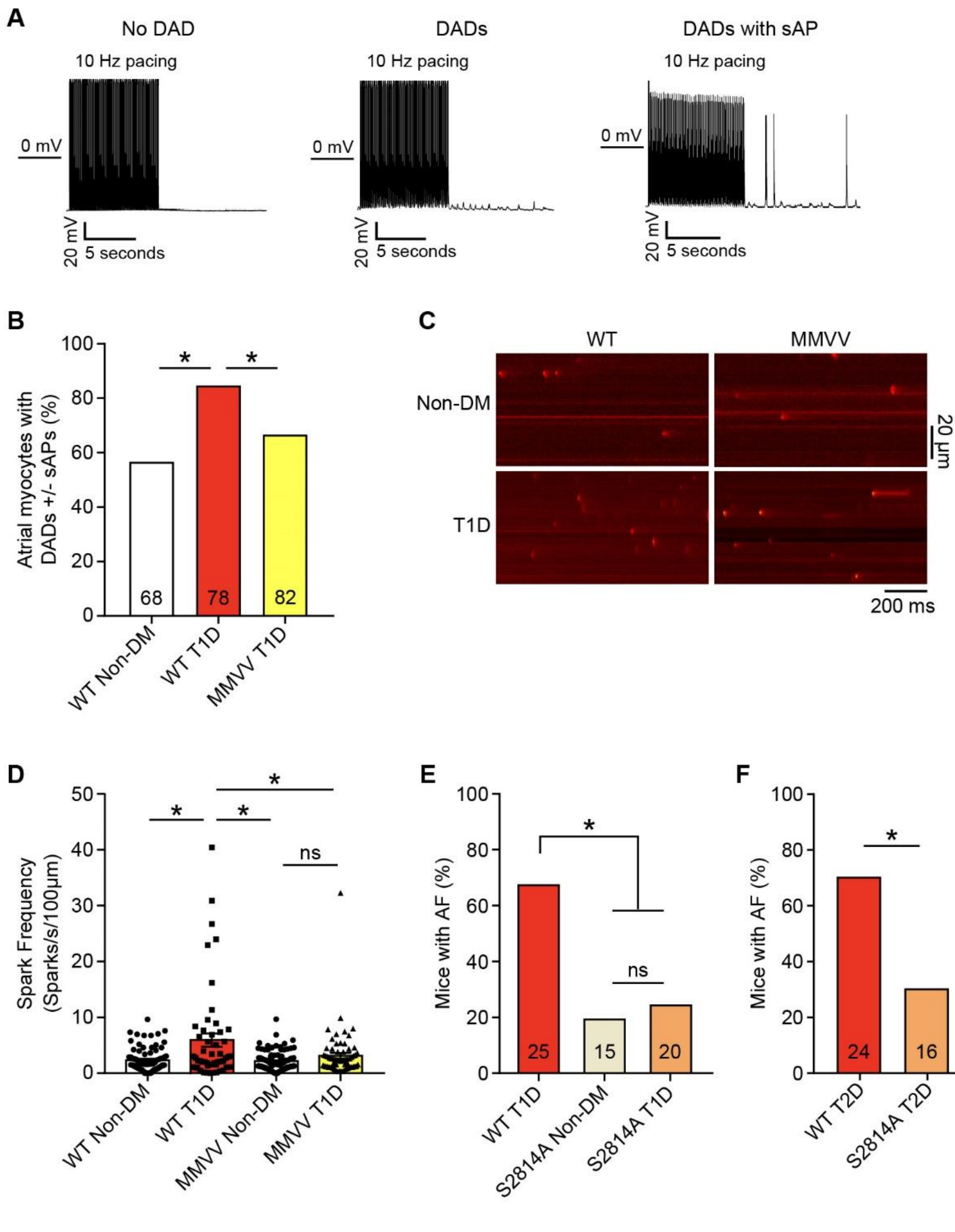

Figure S7. Ox-CaMKII and RyR2 contribute to a proarrhythmic pathway for AF in T1D.
(A) Representative images of delayed after depolarizations (DADs) and spontaneous action potentials (sAP) in response to rapid pacing (10Hz) in isolated atrial myocytes. (B) Summary data for combined percentage frequency of DADs and sAPs in response to rapid pacing of isolated atrial myocytes (n = 4 – 7 mice/group). (C) Representative confocal images and (D) summary data of Ca2+ sparks in atrial myocytes from non-diabetic (non-DM) and T1D WT and MMVV mice (n = 52 – 93 cells from 5 – 7 mice/group). S2814A T1D (E) and T2D (F) mice were protected from AF. Data are represented as percentage frequency distribution (B, E, and F) and mean ± s.e.m (D). Numerals in the bars show total number of cells studied (B) or mice (E and F). Statistical comparisons were performed using two-tailed Fischer's exact test with Holm-Bonferroni correction for multiple comparisons (B, E, and F), one-way AVOVA with Tukey's multiple comparisons test (D). (*$p < 0.05$, ns – not significant). WT T1D (E) and T2D (F) data sets are control data previously presented.

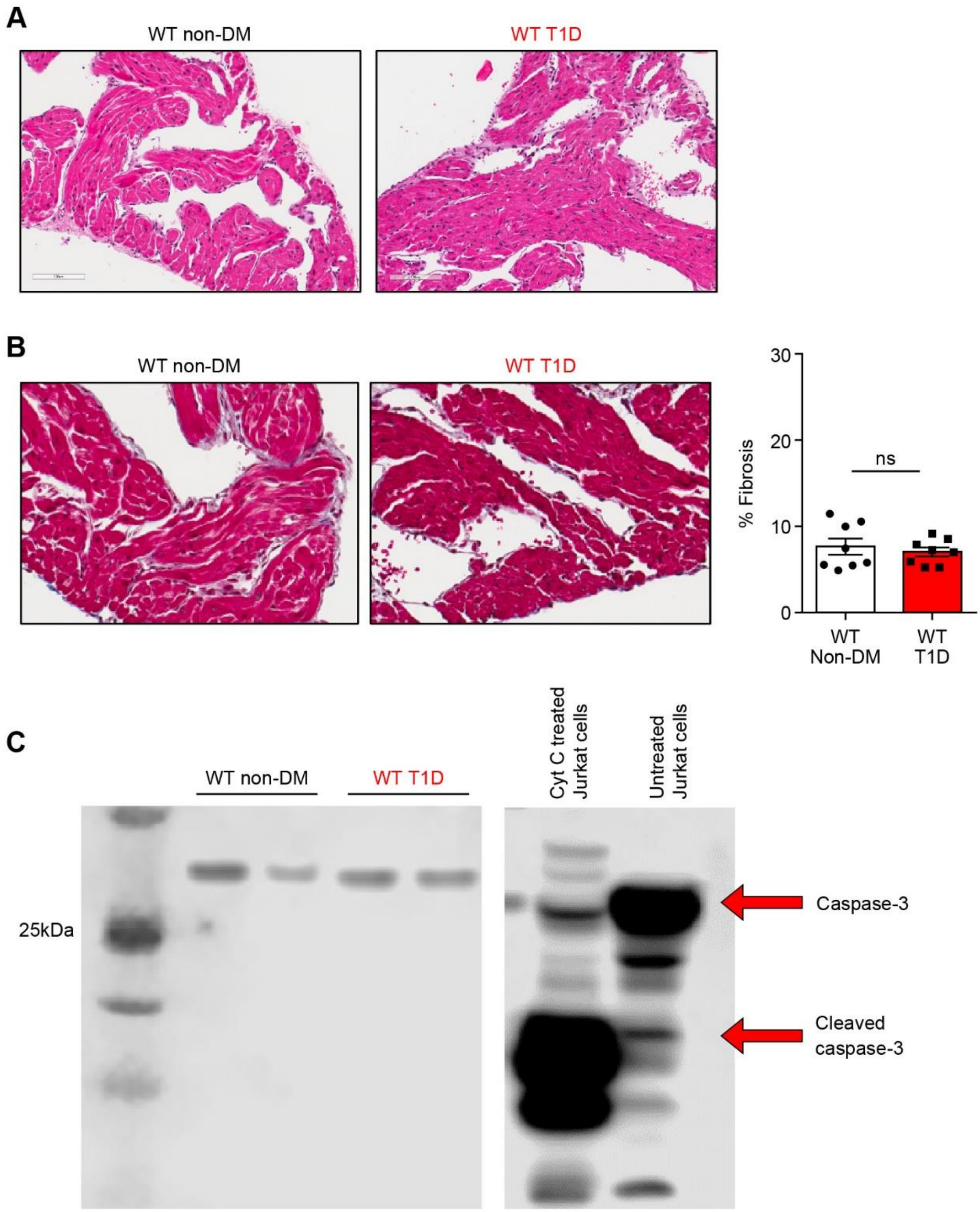

Figure S8. Absence of increased atrial fibrosis or apoptosis in T1D mice
(A) Representative images of hematoxylin and eosin staining of atrial tissue from WT non-DM and WT T1D mice (B) Representative images of Masson's trichrome staining of atrial tissue from WT non-DM (n = 6) and WT T1D (n = 6) mice. There was no increased fibrosis in the T1D mice compared to non-DM mice. (C) Immunoblots for caspase-3 and cleaved caspase-3 in atrial tissue from WT non-DM and WT T1D mice showed no evidence of increased apoptosis in the T1D mice. Cytochrome C treated and untreated Jurkat cells as positive and negative controls respectively for cleaved caspase-3. Cyt C, cytochrome C. Data are represented as mean ± s.e.m., statistical comparisons were performed using two-tailed Student's t test (B). (ns – not significant).